6N01-T5 铝合金焊接接头疲劳断裂分析

刘雪松[1]，　李书齐[1]，　王　苹[1]，　孟立春[2]，　吕任远[2]
（1. 哈尔滨工业大学 先进焊接与连接国家重点实验室，哈尔滨　150001；
2. 南车四方机车车辆股份有限公司，山东 青岛　266000）

刘雪松

摘　要：为了确定 6N01-T5 铝合金挤压型材焊接接头发生疲劳断裂的原因，对 6N01-T5 铝合金型材及其焊接接头分别进行了疲劳试验，获得了它们的 S-N 曲线及条件疲劳极限．分析了接头的显微组织与力学性能，并对疲劳断口进行分析，得到了 6N01-T5 铝合金焊接接头的疲劳断口特征．结果表明，接头显微组织为 α-Al 与 α-Al 和 Mg_2Si 的伪共晶，主要缺欠为气孔；在热影响区与母材交界处存在一软化区，该软化区会引起静载断裂，但不是构件发生疲劳断裂的主要原因；位于焊缝表面焊接缺欠以及构件的表面状态是影响接头疲劳性能的主要原因．

关键词：6N01-T5 铝合金；焊接接头；S-N 曲线；疲劳断裂
中图分类号：TG115.28　　文献标识码：A　　文章编号：0253－360X(2009)10－0025－04

0　序　　言

6N01 铝合金是日本在 20 世纪 80 年代为高速列车开发的用于高速列车车壳的材料，属于 Al-Mg-Si 系铝合金，它首先被应用于 3005 系车辆中[1]．中国于 2002 年成功研制出了第一批高速列车车辆用大型铝合金型材[2]．在车体的制造过程中，国外采用双丝串行 MIG 自动焊和激光-MIG 共熔池焊，有少数国家开始初步尝试搅拌摩擦焊，中国主要采用 MIG 方法进行实际生产的焊接[3,4]．

采用 MIG 方法焊接 6N01 铝合金，会使其焊接接头的疲劳极限降低 40％左右[5]．文中采用 MIG 方法对 6N01-T5 大型铝合金型材进行了焊接，分析了焊接接头的显微组织，进行了硬度、静拉伸和疲劳试验，并对相应的断口进行了分析，综合考察了 6N01-T5 铝合金焊接接头的疲劳性能与其它各种性能之间的关系，为快速获得 6N01-T5 铝合金焊接接头疲劳性能提供了相关的数据．

1　试验方法

试验选用的材料为中国厂家生产的 6N01-T5 铝合金大型挤压型材，型材横截面示意图见图 1，材料基本力学性能见表 1，化学成分见表 2．

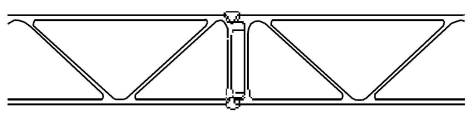

图 1　型材截面示意图
Fig. 1　Cross-section of extrusion

表 1　6N01-T5 铝合金材料的基本力学性能
Table 1　Standard mechanical properties of 6N01-T5 A-alloys

弹性模量 E/MPa	泊松比 μ	抗拉强度 R_m/MPa	条件疲劳极限 σ_a/MPa
6.9×10^4	0.3	120	63.6

表 2　6N01-T5 铝合金及 SAF5356 焊丝化学成分（质量分数，％）
Table 2　Chemical compositions of 6N01-T5 A-alloys and welding wire

材料	Si	Mg	Fe	Mn	Cu	Cr	Zn	Ti	V	Al
6N01-T5	0.60	0.64	0.13	0.110	0.009	0.002 1	0.030	0.034	0.010	余量
SAF5356	0.13	4.90	0.12	0.057	0.011	0.065 0	＜0.130	0.110	—	余量

采用 MIG 方法对型材直接进行焊接，焊接工艺参数为焊接电流 $I=160$ A，焊接速度 $v=75$ cm/min．

收稿日期：2009－06－02
基金项目：教育部博士点基金资助项目（20051059065）

焊后根据分析需要截取相应的试样，对其进行了显微组织分析、硬度试验、静拉伸试验，疲劳试验以及断口分析.

金相试样在焊后的型材上截取，抛光后用混合酸溶液腐蚀(1 mL HF，1.5 mL HCl，2.5 mL HNO_3 和 95 mL H_2O)，而后在 OLYMPUS GX71 金相显微镜下观察. 断口分析的试件直接在拉断的试件上截取，在丙酮溶液中进行超声波清洗后，再进行断口分析. 断口分析的微观观察在 HITACHI S-3400N 扫描电子显微镜下进行. 疲劳试验在低频疲劳试验机上进行，采用轴向拉—拉试验，应力比 $R=0$，加载频率 $f=20$ Hz，循环应力最高加载次数为 10^7 周次. 约定在 10^7 周次循环时仍未起裂的应力范围为条件疲劳极限.

2 试验结果与分析

2.1 焊接接头的显微组织

6N01-T5 铝合金与 SAF5356 焊丝的主要成分为 Al，Mg，Si 三种元素. 熔池凝固时，将首先析出 α-Al. 当温度降低到 α-Al 与 Mg_2Si 的共晶温度 595 ℃时，熔池液体 L 折出 α-Al 与 α-Al 和 Mg_2Si 的伪共晶的混合组织，发生的共晶反应为

$$L \rightarrow \alpha\text{-Al} + Mg_2Si$$

图 2 为 6N01-T5 焊接接头各个部分的组织形貌. 母材是经沉淀强化的 α-Al，主要强化相为 Mg_2Si 相，Mg_2Si 相在金相照片中显示为极细小的黑点. 焊缝中心为等轴晶，焊缝靠近熔合线的部位是沿着温度梯度方向生长的柱状晶. 冷却时，α-Al 与 Mg_2Si 形成的伪共晶最终被排挤到晶界处，在金相照片中显示为深色组织. 与母材的热处理相比，焊缝的冷却速度很快，Mg_2Si 沉淀相析出很少，因此 α-Al 中只能观察到少量的 Mg_2Si 沉淀相. 热影响区与母材组成基本相同，在较快的冷却速度下，只有部分沉淀相能够析出，细小沉淀相的数量明显少于母材. 焊缝中的主要缺欠为气孔，越接近表面，气孔尺寸越大，数量越多. 众所周知，构件的疲劳断裂常起裂于表面或近表面的应力集中处，焊接缺欠是引起应力集中的一个因素. 在实际的生产过程中，一方面受到生产条件的限制，另一方面受到无损检测精度的限制，常允许一定焊接缺欠的存在. 因此，位于焊缝近表面的密集气孔是降低构件疲劳性能的隐患.

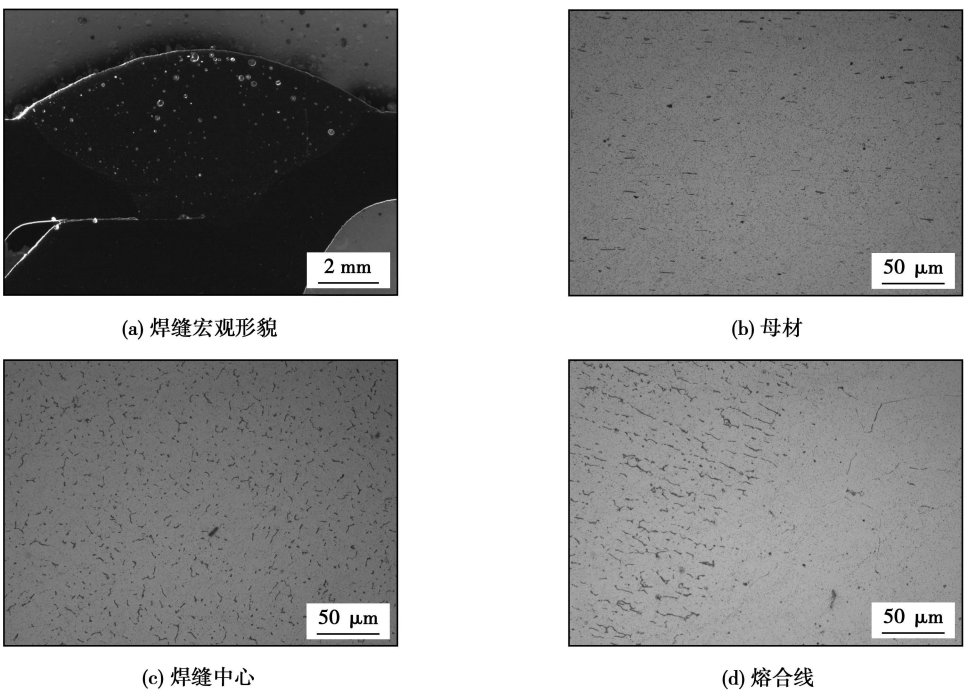

(a) 焊缝宏观形貌　(b) 母材

(c) 焊缝中心　(d) 熔合线

图 2 6N01-T5 焊接接头金相形貌

Fig. 2 Microstructure of 6N01-T5 welding joint

2.2 焊接接头的静力学性能

传统观念认为[6]，铝合金焊接接头疲劳强度下降较大可能是焊接过程引起的热变形和热软化所致，因此考察了 6N01 铝合金焊接接头的抗拉强度与硬度分布特点. 进行硬度测试后发现(如图 3 所示)，在热影响区与母材相邻的位置出现硬度的最低

值，为一软化区．静拉伸试验中，母材的抗拉强度为 265.5 MPa；焊接接头试件全部断裂在该软化区，抗拉强度为 180.1 MPa，是母材抗拉强度的 67.8%．在多种铝合金熔化焊接头中都存在热影响区软化的现象[3,7]．对于时效强化铝合金，产生这种现象的原因是热影响区靠近母材的部位发生过时效，沉淀相长大聚集，沉淀相数目减小，强化效果变差．

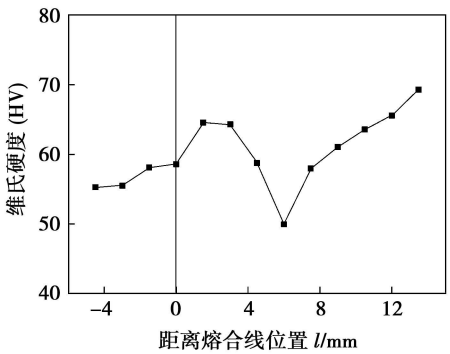

图 3　焊缝的硬度分布

Fig. 3　Hardness distribution of joint

疲劳试验的试件其断裂位置如图 4 所示，可见疲劳断裂与静载断裂不同．在拉断的试件中，疲劳裂纹大多产生在母材与焊缝中，只有 1 个试件断于热影响区．因此热影响区的软化不是焊接接头疲劳性能弱化的主要原因．

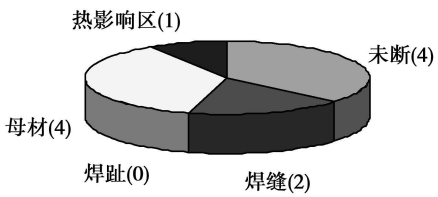

图 4　疲劳试件断裂位置统计

Fig. 4　Statistic of fatigue fracture position

2.3　焊接接头的疲劳性能

根据 S-N 曲线即应力—寿命曲线在双对数坐标系下呈线性关系的假设[8]，将疲劳试验数据在双对数坐标系下进行直线拟合，拟合结果如图 5 所示．求得母材在寿命 $N=10^7$ 周次时对应的条件疲劳极限为 117.5 MPa，焊件在 $N=10^7$ 周次时对应的条件疲劳极限为 70.7 MPa，为母材疲劳极限的 60.2%．

疲劳寿命主要由裂纹的萌生与稳定扩展的时间组成，因此专门考察了断于焊缝和母材试件断口的形貌特点．图 6 分别显示了断在焊缝中心和母材的试件的典型形貌．图6a，b为断于焊缝中心试件的

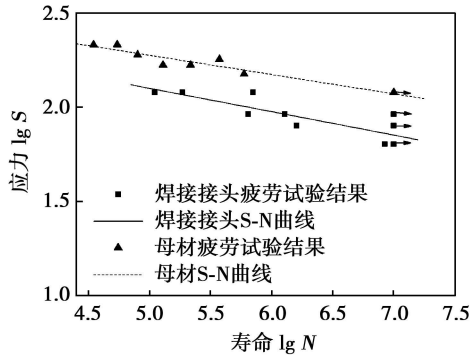

图 5　6N01-T5 焊接接头 S-N 曲线

Fig. 5　S-N curve of welding joint of 6N01-T5 A-alloys

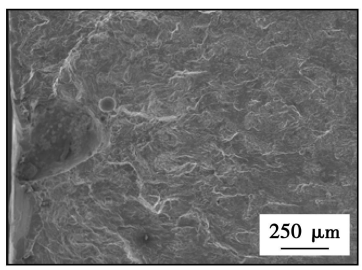

(a) 断于焊接接头的疲劳断口(宏观)

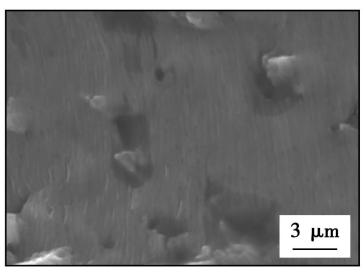

(b) 断于焊接接头的稳定扩展区疲劳辉纹

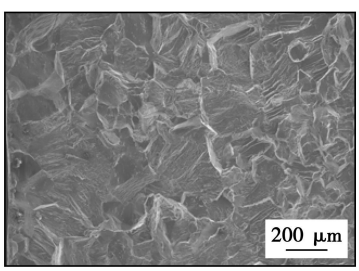

(c) 断于母材的疲劳断口(宏观)

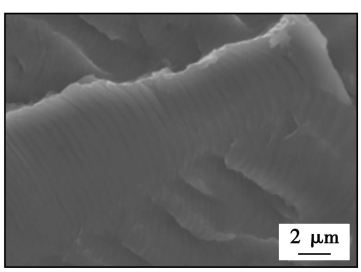

(d) 断于母材的稳定扩展区疲劳辉纹

图 6　焊接接头疲劳断口形貌

Fig. 6　Fatigue fracture apperance of welding joint

疲劳断口形貌特点. 疲劳裂纹起裂于表面的大气孔,稳定扩展区完全由小片状解理面组成,与 Al-Mg-Si 系铝合金在欠时效状态下的疲劳断口稳定扩展区形貌相似[9]. 将稳定扩展区放大到 5 000 倍左右时,可观察到清晰的疲劳辉纹,疲劳辉纹被解理台阶和第二相截断成小段,且疲劳辉纹的间距随着远离源区逐渐增大. 由于晶粒中沉淀相较少,位错在运动时受到的阻力较小,滑移系启动所需能量较小;因此裂纹扩展时,裂纹尖端附近的塑性储备易达到几个滑移系同时被激活所需要的能量,符合疲劳裂纹按第二阶段扩展方式扩展的条件,在一个或者几个载荷的作用下,形成一条疲劳辉纹. 随着裂纹的扩展,试件的承载面积逐渐减小,相应地,所受到的载荷逐渐增大,这直接导致疲劳辉纹的间距逐渐增大. 图 6c, d 所示为断于母材试件的疲劳断口形貌特点. 整个断口与母材疲劳断口形貌特点一致,整体表现为沿晶与解理的混合形貌,在少数的解理面上可以观察到细密的疲劳辉纹,在源区可见极窄长的刻痕,表明裂纹起裂在表面刻痕处.

对接焊件产生应力集中的原因有焊趾处的几何形状突变、焊缝表面及近表面的焊接缺欠以及焊件表面状态. 疲劳断口的分析表明,后两者是引起试验批次试件发生疲劳断裂的主要原因.

3 结 论

(1) 对 6N01-T5 焊接接头进行了综合性能评价,焊缝成形良好,主要缺欠是位于表面或近表面的气孔,在热影响区存在由于过时效而产生的软化区,其抗拉强度为母材的 67.8%. 通过疲劳试验,得到母材的条件疲劳极限为 117.5 MPa,焊接接头的条件疲劳极限为 70.7 MPa,为母材的 60.3%.

(2) 通过对比静载试件与疲劳试件断裂位置确定,由于焊接而产生的热影响区软化不是造成焊接接头疲劳性能下降的主要原因.

(3) 试验试件断裂位置的统计以及断口分析结果表明,焊缝表面及近表面的气孔以及构件的表面状态是使焊接接头发生疲劳断裂的主要原因.

参考文献:

[1] 刘静安. 日本大断面铝合金挤压型材生产技术[J]. 铝加工, 1995, 18(5): 17—22.
Liu Jingan. Large section aluminum alloy extrusion technology in Japan [J]. Aluminium Fabrication, 1995, 18(5): 17—22.

[2] 刘静安. 6005A 铝合金大型特种型材的研制[J]. 轻合金加工技术, 2004, 32(4): 36—41.
Liu Jingan. The extrusion of large sized special 6005A aluminium profile[J]. Light Alloy Fabrication Technology, 2004, 32(4): 36—41.

[3] Moreira P M G P, de Figueiredo M A V, de Castro P M S T. Fatigue behaviour of FSW and MIG weldments for two aluminum alloys[J]. Theoretical and Applied Fracture Mechanics, 2007, 48(2): 169—177.

[4] Yonetani H. Laser-MIG hybrid welding to aluminium alloy carbody shell for railway vehicles[J]. Welding International, 2008, 46(2): 43—47.

[5] 王元良, 骆德阳, 王一戎. 我国高速列车焊接技术及其新发展[J]. 电焊机, 2008, 38(8): 8—12.
Wang Yuanliang, Luo Deyang, Wang Yirong. Welding and its development of bullet train[J]. Electric Welding Machine, 2008, 38(8): 8—12.

[6] 方洪渊. 焊接结构学[M]. 北京: 机械工业出版社, 2008.

[7] 尹志民, 张爱琼, 王炎金. 6005A 铝合金型材焊接接头组织与性能[J]. 轻合金加工技术, 2001, 29(1): 32—34.
Yin Zhimin, Zhang Aiqiong, Wang Yanjin. Microstructure and properties of welded joint of extruded 6005A aluminium alloy[J]. Light Alloy Fabrication Technology, 2001, 29(1): 32—34.

[8] 赵少汴. 抗疲劳设计[M]. 北京: 机械工程出版社, 1994.

[9] Jiang D, Wang C. Influence of microstructure on deformation behavior and fracture mode of Al-Mg-Si alloys[J]. Materials Science & Engineering A, 2003, 352(1—2): 29—33.

作者简介: 刘雪松, 男, 1968 年出生, 博士, 副教授, 硕士生导师. 主要从事焊接结构与可靠性评价方面的科研和教学工作. 发表论文 50 余篇.

Email: liuxuesong@hit.edu.cn

Comparison of joint performance between weld-bonding and resistance spot welding of dual-phase steel SUN Haitao, ZHANG Yansong, LAI Xinmin, CHEN Guanlong (Shanghai Key Laboratory of Digital Autobody Engineering, Shanghai Jiaotong University, Shanghai 200240, China). p 17—20

Abstract: The joint performances between weld-bonding and resistance spot welding (RSW) are compared by tensile-shear force of nuggets, microstructure of nuggets, dynamic resistance curves and weld lobes. Experimental results show that the tensile-shear force of weld-bonded nuggets is much higher than that of spot-welded nuggets when lower welding current is used; oppositely tensile-shear force of spot-welded nuggets is a little higher than that of weld-bonded nuggets when higher welding current is used, but severe spatter will occur. Therefore, lower welding current in weld-bonding of steel comparing with that of RSW and larger electrode force during welding will inhibit spatter.

Key words: weld-bonding; resistance spot welding; dual-phase steel; joint performance

Fuzzy synthetical evaluation of weld bead stability for pulse MAG welding prototyping MENG Fanjun[1], ZHU Sheng[2], DU Wenbo[2] (1. Department of Remanufacturing Engineering, The Academy of Armored Forces Engineering, Beijing 100072, China; 2. National Key Laboratory for Remanufacturing, The Academy of Armored Forces Engineering, Beijing 100072, China). p 21—24

Abstract: Hierarchy analytical theory combined with the experiment is employed to determine the weld bead stability synthesis evaluation weight coefficient of weld surface quality, weld reinforcement and weld width of weld bead. The membership degree tables of surface quality, weld reinforcement and weld width are created by fuzzy theory. The analytic hierarchy theory and the fuzzy mathematics are applied to evaluate practical bead stability. The results show that the calculation value accords with the actual result, which proves the method of bead stability evaluation is effective.

Key words: weld bead stability; hierarchy analytical theory; fuzzy evaluation

Fatigue failure analysis of 6N01-T5 aluminum alloy welded joints LIU Xuesong[1], LI Shuqi[1], WANG Ping[1], MENG Lichun[2], LÜ Renyuan[2] (1. State Key Laboratory of Advanced Welding & Joining, Harbin Institute of Technology, Harbin 150001, China; 2. CSR Sifang Locomotive and Rolling Stock, Co. Lt, Qingdao 266000, China). p 25—28

Abstract: To identify the main cause of fatigue failures of welded joints of 6N01-T5 aluminum alloy extrusions, fatigue tests were carried out upon 6N01-T5 aluminum alloy extrusions and their weld joints, and S-N curves and conditional fatigue limits of them were obtained. Microstructure and mechanical properties of the welded joints were investigated. The fatigue fractures of the joints were analyzed and thereby the characteristics of them were obtained. The results show that the microscopic structure of the joints is α-Al and pseudo eutectic made up of α-Al and Mg_2Si; the defects of the joints are mainly gas cavities; there is a soften zone between HAZ and base metal which lead to fracture under dead-load but hardly to fracture failure; the main influence factors of fatigue performance are defects on the surface of weld and the surface condition of the weldment.

Key words: 6N01-T5 aluminum alloy; welded joints; S-N curve; fatigue failure

Corrosion resistance of intermediate temperature filler metal for stepped welding to 6063 aluminum alloy ZHU Hong[1,2], XUE Songbai[1], SHENG Zhong[1] (1. College of Materials Science and Technology, Nanjing University of Aeronautics and Astronautics, Nanjing 210016, China; 2. 14th Research Institute, China Electronic Technology Group Corporation, Nanjing 210013, China). p 29—32

Abstract: The effects of contents of Si, Cu, Ni and RE on the corrosion potential, weightlessness and corrosion rate of Al-Si-Cu-Ni-RE filler metal were studied by using orthogonal test, and the microstructure of the corroded filler metal was analyzed by means of SEM and EDS. It is indicated that the corrosion potential of the filler metal is relative to its weightlessness, which with the increase of the negative value of corrosion potential, the weightlessness increases continuously. Based on the corrosion rates, the results show that Ni has the most important influence on the melting points, and then do Si, Cu and RE. Through observed and analyzed the microstructure of filler metal, it is found that the matrix phase α (Al) with face-centered cubic solid solution makes the performance of joint better, but black brittle phase θ (Al_2Cu) makes the performance of joint poorer; Cl^- is the prime cause of induced pitting corrosion of the filler metal, which the pitting corrosion in filler metal and the obvious inter-granular corrosion are found in local area after corrosion.

Key words: orthogonal test; corrosion rate; pitting; inter-granular corrosion

Microstructure of magnesium alloy joints in resistance spot welding LANG Bo[1], SUN Daqian[2], REN Zhenan[2], ZHU Baiqing[3] (1. Beijing Aeronautical Manufacturing Technology Research Institute, Beijing 100024, China; 2. School of Materials Science and Engineering, Jilin University, Changchun 130025, China; 3. Beiqi Foton Motor Co., Ltd, Beijing 102206, China). p 33—36, 40

Abstract: The microstructure and phase composition of magnesium alloy joints in resistance spot welding are investigated with optical microscopy, confocal laser scanning microscope and X-ray diffraction for improving mechanical properties of the joints. The results show that the joints consist mainly of weld nugget and heat-affected zone (HAZ). The weld nugget contains two different structures, the cellular-dendritic structure at the edge of the nugget and the equiaxed dendritic structure in the center of the nugget. The weld nugget consists of α-Mg phase and a small amount of β-$Mg_{17}Al_{12}$ phase. Comparing with the grains in no melting base metal, the